

# BEAM COMMISSIONING OF THE NEW DIGITAL LOW-LEVEL RF SYSTEM FOR CERN'S AD

M. E. Angoletta<sup>†</sup>, S. Albright, D. Barrientos, M. Jaussi, A. Findlay, A. Rey, M. Suminski  
 CERN, Geneva, Switzerland

## Abstract

CERN's Antiproton Decelerator (AD) has been re-furnished and equipped with a new digital Low-Level RF (LLRF) system, successfully commissioned in 2021.

The new LLRF system routinely captures and decelerates more than  $3E7$  antiprotons from 3.5 GeV/c to 100 MeV/c in successive steps, interleaved with cooling periods. It implements the frequency program, beam phase/radial and cavity amplitude/phase feedback loops. An extraction synchronization loop allows transferring a bunch of antiprotons to the Extra Low Energy Antiproton ring (ELENA). The LLRF parameters are controlled by a dedicated application and operational modes such as bunched beam cooling have been successfully deployed.

This paper gives an overview of the LLRF commissioning and challenges. Hints on future steps are also provided.

## INTRODUCTION

CERN's Antiproton Decelerator (AD) has been re-furnished to provide reliable operation to the Extra Low Energy Antiproton ring (ELENA), now its sole user. Upgrades included replacing the ferrite-based decelerating High-level RF (HLRF) system with one based on Finemet® alloy. A new Low-Level RF (LLRF) system was commissioned in 2021 to carry out beam and cavity loops.

Table 1 shows the momentum and revolution frequency values at each flat-top. Figure 1 shows the typical AD production cycle and its RF segments, i.e. cycle parts where the RF is active. The current cycle duration is 115 s.

Table 1: AD Flat-top Momentum and Frequency Values

Flat-top	Momentum	Revolution frequency
FT1	3.57 GeV/c	1.589478 MHz
FT2	2 GeV/c	1.487728 MHz
FT3	300 MeV/c	500.465 kHz
FT4	100 MeV/c	174.155 kHz

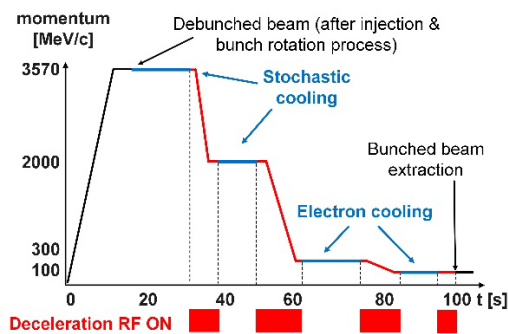


Figure 1: AD production cycle.

<sup>†</sup> maria.elena.angoletta@cern.ch

## LLRF OVERVIEW

### Layout

The AD LLRF belongs to the LLRF family operational in several CERN machines [1] and is a customised version of the ELENA LLRF [2]. Figure 2 shows a schematic view of the system and of its available functionalities. An initial description is available elsewhere [3]; here only previously un-mentioned features are outlined.

One Highland V346 waveform generators module, hosted in a separate VME crate and controlled by the AD LLRF, gives the reference to the AD extraction synchronisation loop. Harmonics of this signal provide timings to the AD extraction/ELENA injection kickers as well as the ELENA LLRF injection reference. The same module generates fixed trains at the flattops frequencies used by spectrum analysers for cooling setup. A remotely controlled programmable amplifier increases the signal level within the cycle for debunched beam data acquisition/analysis.

### System Operation

The AD beam is decelerated in successive steps, called RF segments. The four segments now used in operation are shown in red in Figure 1; different segments can be used for test purposes. The beam is adiabatically bunched at the start of each segment and is debunched at its end. An exception is the last segment where an extraction synchronisation loop permits extracting a single bunch to ELENA. Beam phase/radial loops stabilise the beam and keep it in the centre of the pipe. A voltage/phase cavity loop maintains the desired voltage in the cavity. The sampling period of the digital loop is 12.5  $\mu$ s thus allowing a satisfactory bandwidth of several kHz. Features such as deceleration harmonic number, voltage program and loop gains are defined and loaded onto the LLRF on a "per segment" basis. Other operational modes such as bunched beam cooling and bunch rotation at extraction are available.

## LLRF BEAM COMMISSIONING

### Overview

The AD LLRF commissioning planning included 13 working days in July 2021, interleaved with cooling commissioning periods. The cooling commissioning was longer than expected hence the overall AD LLRF commissioning overflowed into ELENA's one. Antiproton physics was started timely on August 24<sup>th</sup>, 2021 whilst setup activities continued for one more month.

Four weeks of beam commissioning were allocated to AD/ELENA in April 2022 to restart the machines after the winter shutdown. This second commissioning slot allowed us to deploy new features devised during the 2021 run.

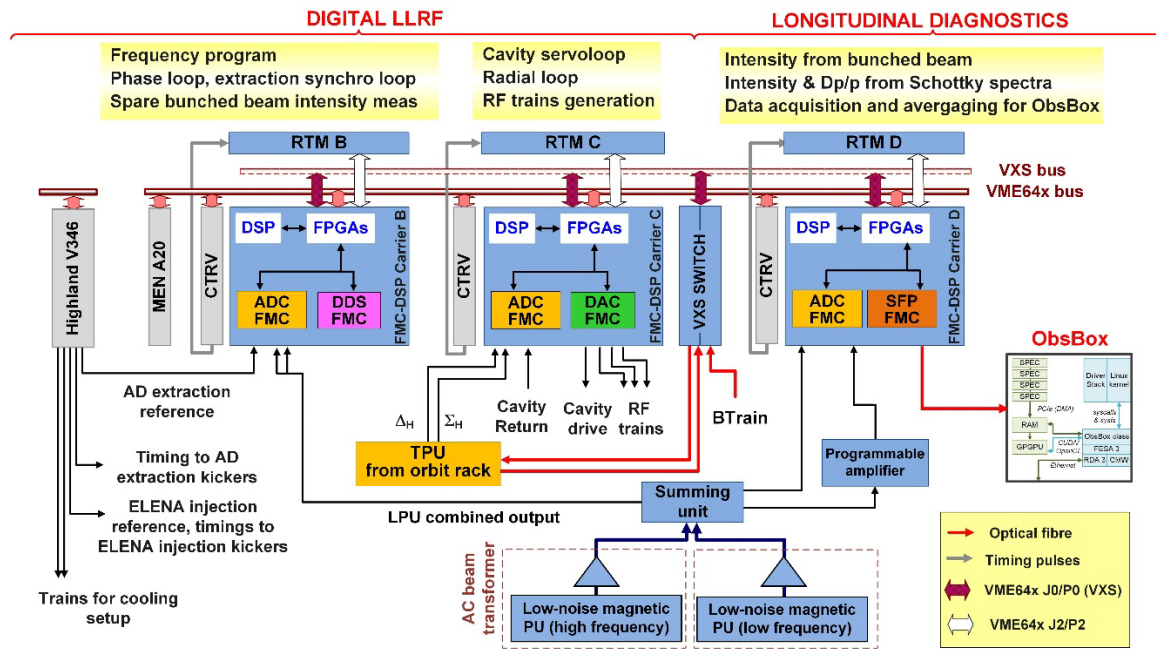


Figure 2: AD LLRF and longitudinal diagnostics. Keys: FMC – FPGA Mezzanine Card, DDS – Direct Digital Synthesiser, ADC – Analogue-to-Digital Converter, DAC – Digital-to-Analogue Converter, SFP – Small Form-factor Pluggable Transceiver, LPU/TPU – Longitudinal/Transverse Pick-Up, CTRV – Timing Receiver Module, MEN A20 – Master VME board, RTM – Rear Transition Module, ObsBox – custom acquisition/processing module, SPEC – Simple PCI Express carrier module, Highland V346 – waveform generator module.

### HLRF Operation

The LLRF implements a digital servoloop at the deceleration harmonic. The servoloop is based on [I,Q] coordinates and has a bandwidth of some kHz, well adapted to AD operation. Table 2 shows the maximum voltage profile the LLRF permits as a function of frequency. A high-to-low voltage transition window avoids steps in the voltage program which could cause the loop response to overshoot.

The LLRF controls in real time a gap relay that short-circuits the HLRF during cooling periods to avoid interfering with them. The gap relay takes about 84 ms to change status. In the 2021 run a strong line was visible at the RF frequency on cooling actions for AD’s lower plateaus. The installation of one additional gap relay in 2022 reduced this effect. More investigations are under way.

Table 2: HLRF Voltage as a Function of Frequency

Frequency range [kHz]	Max Voltage [Vpeak]
2000 - 500	3500
500 - 480	Decreases linearly 3500 V → 500 V
480 – 145	500
Elsewhere	0

### RF Harmonics

The decelerating harmonic  $h$  selectable in an RF segment depends on the frequency range and on the corresponding HLRF voltage profile. The preferred scheme was to use  $h = 1$  on all segments apart from the third one (300 to 100 MeV/c), where  $h = 3$  was foreseen. Unfortunately,

the upgraded orbit system could not cope with a harmonic change in 2021 hence a deceleration at  $h = 1$  only was carried out. The measurement problem was later solved and we now decelerate at  $h = 3$  on the third RF segment.

### Frequency Correction and Loops Contribution

The Btrain value received by the LLRF to compute the frequency program is simulated. Inaccurate values and imprecise magnet current regulation require adding a correction to the frequency program during the cycle. This allows the LLRF to deposit the beam at the correct energy at the end of an RF segment and to capture it properly after the cooling step. Figure 3 shows the frequency correction and the contributions from various loops for a typical AD cycle.

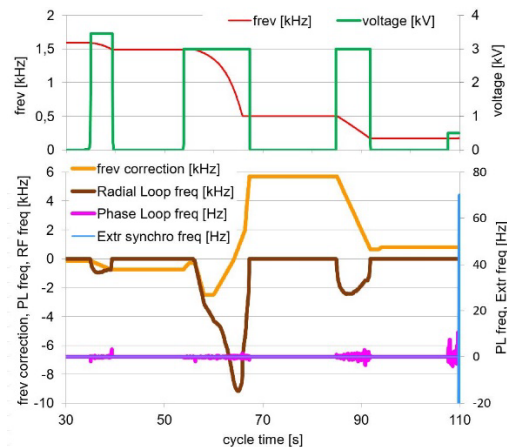


Figure 3: Upper plot: voltage program and revolution frequency. Lower plot: frequency correction function and loops contribution. The horizontal scale is the cycle time.

Content from this work may be used under the terms of the CC BY 4.0 licence (© 2022). Any distribution of this work must maintain attribution to the author(s), title of the work, publisher, and DOI

The new LLRF implements a beam radial loop, previously unavailable. The input for the radial loop is the orbit position calculated in real time by the orbit system and transferred to the LLRF via optical fibre.

### LLRF Setup

Contrary to other machines, the AD cycle length can change for example to accommodate longer cooling periods. LLRF parameters such as timings, harmonics and functions are automatically adapted to the new requirements, avoiding manual intervention of an RF expert. This is carried out by the AD cycle editor and by the AD RF cycle editor. Figure 4 shows the RF cycle editor available since 2022. The lines corresponding to the four operational segments are highlighted in red and depend on the underlying, complex AD cycle structure (“ELTAG” column). The editor allows setting the deceleration voltage (“Voltage H1” column) as well as its adiabatic changes (“Threshold H1” column). The decelerating harmonic is given in the “Harmonic” column together with the rotation parameters (“Phase H1” and “Delay H1” columns) used to calculate the cavity-to-beam phase, which is the phase loop input. The rotation values on the first line are used when an RF segment comprises several lines in the editor. The execution of a bunch rotation prior to extraction can be enabled.

ELTAG	Momentum	Seg. Delay	Voltage H1	Threshold H1	Harmonic...	Phase H1	Delay H1
RMP1		0.0	0.0	0	1	0.0	0.0
FT1	3574	0.0	0.0	0	1	0.0	0.0
RMP2		0.0	3500.0	2.5	1	-55	-78
FT2A	2000	0.0	100.0	1	1	0.0	0.0
RMP3		0.0	3000.0	10.0	1	-13	-155
FT2B	1999	0.0	3000.0	0	1	0.0	0.0
RMP4		0.0	3000.0	0	1	0.0	0.0
FT3A	300	0.0	3000.0	0	1	0.0	0.0
RMP5		0.0	3000.0	0	1	0.0	0.0
FT3B	300	0.0	0.0	2.0	1	0.0	0.0
RMP6		0.0	0.0	0	1	0.0	0.0
FT3C	300	0.0	0.0	0	1	0.0	0.0
RMP7		0.0	3000.0	0.1	3	-50	-450
FT4A	100	0.0	0.0	0.15	1	0.0	0.0
RMP8		0.0	0.0	0	1	0.0	0.0
FT4B	100	0.0	0.0	0	1	0.0	0.0
RMP9		-2341.0	500.0	0.15	1	0.0	0.0
FTSP3	50	0.0	0.0	0	1	0.0	0.0

Figure 4: RF cycle editor from the 2022 AD run.

The RF cycle editor sets two LLRF timings per segment to define the “End capture” and “Start debunching”. It also sets the “Start RF segment” and “End RF segment” timings according to the selected adiabatic voltage changes. The LLRF timings are derived from these timings. Examples are the timings to start/stop the phase (SPL/EPL) and the radial (SRL/ERL) loops. This mechanism allows to load all new LLRF segment parameters (INCYINIT) and the gap to open (SOPENGAP) before voltage is requested from the HLLRF. Figure 5 shows the general mechanism of timing control in a segment. Other timings required for the hardware setup specific to each RF segment are not shown.

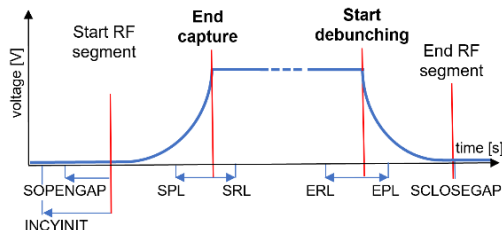


Figure 5: LLRF timings control by RF cycle editor.

## LLRF COMMISSIONING CHALLENGES

The AD cycle is composed of interleaved deceleration and cooling periods. The AD commissioning is thus inherently sequential as each RF segment can be setup only once the preceding cooling step is operational. The AD cycle lasts about 2 minutes, hence data observation is slow.

The 2021 AD commissioning occurred in summer and experts were often unavailable. Furthermore, it happened in parallel with the restart or operation of other systems supported by the same team.

The AD LLRF commissioning however profited heavily from experience in its twin machine ELENA, whose commissioning was started in 2017 and where the main LLRF features were first deployed and validated.

## INITIAL BEAM ACHIEVEMENTS

AD extracts routinely to ELENA a single bunch of about 3 E7 antiprotons. The post-upgrade AD deceleration efficiency reaches 87% and is similar or better than what was previously achieved.

The AD cycle lasts five seconds longer than before the upgrade. This is partially due to the deceleration carried out at  $h = 1$  in all RF segments owing to the initial orbit system limitations. In 2022 we could operate at harmonic  $h = 3$  on the third segment. This will allow cycle shortening.

Figure 6 shows a tomogram [4] of the bunch at extraction in 2021 and after bunched beam cooling. A satisfactory bunch length of 170 ns for 2.1 E7 particles was obtained.

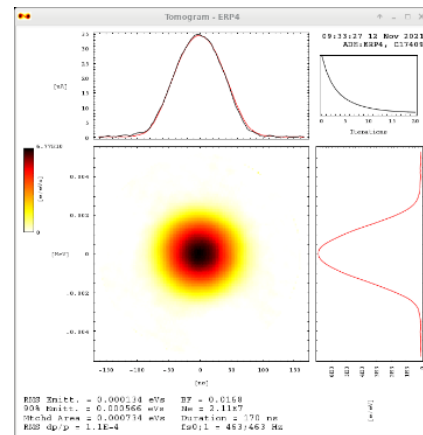


Figure 6: Beam tomogram before extraction.

## CONCLUSIONS AND FUTURE WORK

The commissioning of the new AD LLRF was challenging but successful: antiproton physics started as planned and the LLRF system worked reliably. New desired features, identified in the 2021 run, were deployed in 2022.

Future work to further optimise the system setup and to improve the diagnostics capabilities, especially bunched/debunched beam parameter measurements, is planned.

## ACKNOWLEDGEMENTS

The authors are grateful to the whole AD operation crew for their constant support in operating the LLRF. Thanks also to D. Gamba for useful discussions and suggestions.

## REFERENCES

- [1] M. E. Angoletta *et al.*, "Achievements and New Challenges for CERN's Digital LLRF Family", LLRF19 workshop, Chicago, USA. doi:10.48550/arXiv.1910.06643
- [2] M. E. Angoletta, M. Jaussi, and J. C. Molendijk, "The New Digital Low-Level RF System for CERN's Extra Low Energy Antiproton Machine", in *Proc. IPAC'19*, Melbourne, Australia, May 2019, pp. 3962-3965. doi:10.18429/JACoW-IPAC2019-THPRB069
- [3] M. E. Angoletta, S. C. P. Albright, A. Findlay, M. Jaussi, J. C. Molendijk, and V. R. Myklebust, "A New Digital Low-Level RF and Longitudinal Diagnostic System for CERN's AD", in *Proc. IPAC'19*, Melbourne, Australia, May 2019, pp. 3966-3969. doi:10.18429/JACoW-IPAC2019-THPRB070
- [4] S. Hancock, S. R. Koscielniak, M. Lindroos, "Longitudinal Phase Space Tomography with Space Charge", *Physical Review Special Topics – Accelerators and Beams*, vol. 3, p. 124202, 2000. doi:10.1103/PhysRevSTAB.3.124202